



Solubility of water in pyrope-rich garnet at high pressures and temperature

Mainak Mookherjee¹ and Shun-ichiro Karato²

Received 7 October 2009; revised 25 November 2009; accepted 22 December 2009; published 12 February 2010.

[1] The water solubility in pyrope-rich garnet was determined between pressures of 5–9 GPa and temperatures of 1373–1473 K under silica activity and oxygen fugacity similar to those expected in the Earth's upper mantle. We found that pyrope-rich garnet has substantial water solubility up to ~ 0.1 wt% under these conditions. In addition, the water content in garnet varied as a function of chemical conditions. In particular, the variation in water fugacity (and Mg#) caused a variation in water partitioning with olivine ($D_{H_2O}^{ol/py}$). The substantial water solubility in pyrope-rich garnet under deep upper mantle conditions might have significant influence on physical and transport properties. **Citation:** Mookherjee, M., and S. Karato (2010), Solubility of water in pyrope-rich garnet at high pressures and temperature, *Geophys. Res. Lett.*, 37, L03310, doi:10.1029/2009GL041289.

1. Introduction

[2] Trace amounts of hydrogen dissolved as defects in nominally anhydrous mantle phases affect melting temperature [Kushiro *et al.*, 1968], elasticity [Jacobsen and Smyth, 2006], rheology [Mackwell *et al.*, 1985], electrical conductivity [Dai and Karato, 2009a] and deformation fabrics [Jung and Karato, 2001]. An important step in understanding the role of hydrogen is to determine the solubility limit and solubility mechanisms in these mantle minerals. Extensive studies have been conducted on the solubility of hydrogen in major mantle minerals such as olivine [Kohlstedt *et al.*, 1996], orthopyroxene [Mierdel *et al.*, 2007], wadsleyite and ringwoodite [Kohlstedt *et al.*, 1996] and clinopyroxene [Bromiley *et al.*, 2004]. Based on these studies, the water storage capacity in the upper mantle and transition zone has been estimated [Hirschmann *et al.*, 2005]. Constraints on the water content in these regions were also inferred based on the results of electrical conductivity measurements on olivine [Wang *et al.*, 2006], orthopyroxene [Dai and Karato, 2009b], wadsleyite and ringwoodite [Dai and Karato, 2009c; Huang *et al.*, 2005]. However, these studies are incomplete since these minerals occupy only ~ 40 – 80% of these regions, and the robustness of results of these studies hinges upon the degree to which the remaining mineral phases influence the hydrogen solubility and distribution. Among these, garnet is the most important secondary mineral whose volume fraction ranges from $\sim 20\%$ in the shallow upper mantle for the

pyrolite model to $\sim 80\%$ in the transition zone for the piclogite model.

[3] Although being an important phase, there is little consensus on the solubility and dissolution mechanisms of hydrogen in garnet. Under deep upper mantle conditions ($P > 7$ GPa), [Withers *et al.*, 1998] concluded that there was virtually no hydrogen soluble in pyrope, whereas Lu and Keppler [1997] observed small but finite hydrogen solubility (~ 200 ppm wt of H₂O). Earlier, [Geiger *et al.*, 1991] also investigated the hydrogen content in synthetic pyrope at $P = 2$ – 5 GPa and $T = 1073$ – 1273 K and obtained the water solubility of ~ 200 – 700 ppm wt. The values of hydrogen solubility at low pressures reported by these papers differ by as much as a factor of ~ 5 . The main purpose of this article is to provide constraints on the water contents in garnet at high pressures and temperature, documenting the role of chemistry and chemical environment relevant to upper mantle conditions.

2. Method

[4] Starting materials consisted of a single crystal of pyrope-rich garnet (Table S1) cut into cubes of dimension $0.5 \times 0.5 \times 0.5$ mm³ and an oriented San-Carlos olivine single-crystal of dimension $0.7 \times 0.8 \times 0.9$ m³.¹ These single crystals were placed in an inner nickel capsule and an outer platinum capsule, which was sealed by welding (Figure 1a). Silica activity was buffered by a mixture of olivine, orthopyroxene and clinopyroxene powder. A mixture of talc and brucite in the ratio 1.4:1 by weight was used as a water source. The water content of the olivine crystals was used to estimate the water fugacity and the degree of saturation of the sample environment during each annealing run. The high-pressure annealing experiments were carried out in a 1000 ton Kawai type multi-anvil apparatus between pressures of 6–9 GPa. Experiments were mostly carried out at 1373 K (Table 1). The temperature was increased at 50 K/min after the experimental pressure was reached in order to minimize the loss of water from the capsule. Most samples were held at annealing temperature and pressures for 5 to 24 hrs. The compositions of the recovered phases were analyzed by JEOL 8900 electron microprobe using four wavelength dispersive spectrometers (Table S1). Trace quantities of Li and B were detected using Laser-ablation inductively-coupled-plasma mass-spectrometer (LA-ICPMS) facility at Misasa, Japan. The lithium (Li₂O) content is of the order of 0.18 ppm wt and the boron (B₂O₃) content is of the order of 0.08 ppm wt.

¹Bayerisches Geoinstitut, University of Bayreuth, Bayreuth, Germany.

²Department of Geology and Geophysics, Yale University, New Haven, Connecticut, USA.

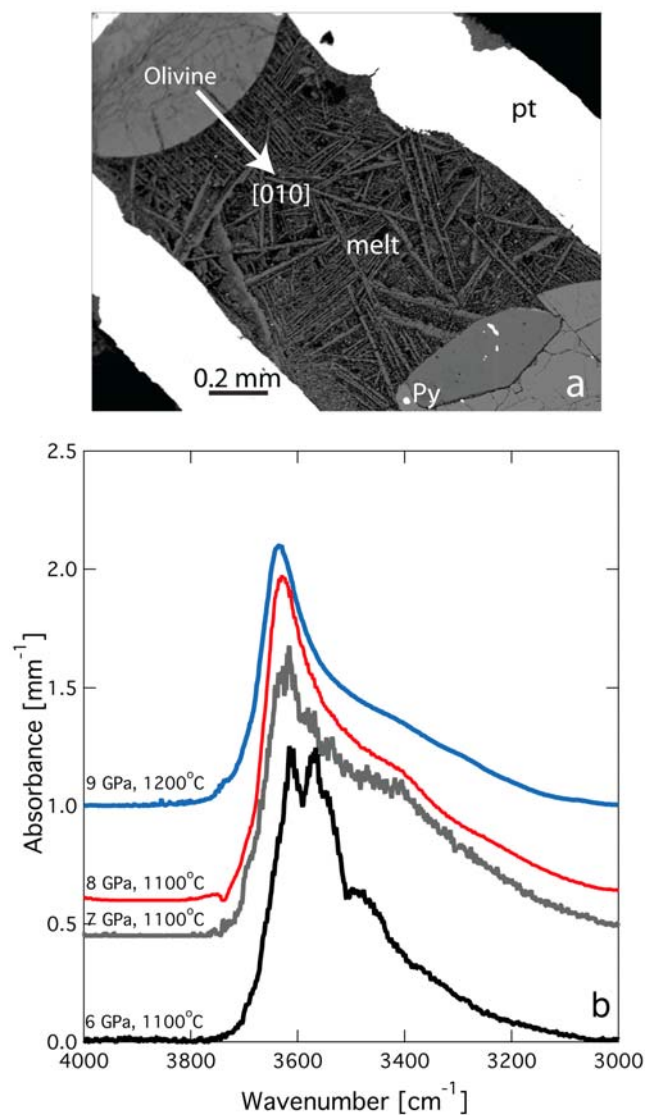


Figure 1. (a) Back scattered electron (BSE) image of pyrope-rich single crystal (py), quenched melt, and olivine single crystal (K670). The [010] direction of olivine single crystal is oriented along the arrow. The orientation is determined by electron back scattered diffraction (EBSD) method. The quenched crystals (melt) indicate coexistence of hydrous mafic melt with olivine and garnet. (b) FTIR spectra of garnet crystal, annealed at different pressures. Most spectra have an asymmetric peak centered at around $\sim 3630\text{ cm}^{-1}$. At low-pressures, additional bands occur at 3615, 3566, and 3496 with shoulders at $\sim 3545\text{ cm}^{-1}$. The broad absorption at $\sim 3367\text{ cm}^{-1}$ might be related to O-H...O interaction between the hydroxyl and oxygen atoms in the crystal structure.

[5] To determine the water content, Fourier-transformed infrared absorption spectra were collected on doubly polished thin sections ($\sim 100\text{ }\mu\text{m}$ thick) using unpolarized radiation and a minimum spot size of $30\text{ }\mu\text{m}$. Garnet has cubic symmetry and therefore we have used unpolarized radiation. The absorption spectra showed no evidence of

saturation. The absorption coefficient of $\epsilon = 6700 \pm 670\text{ (Lmol}^{-1}\text{ cm}^2)$ [Bell *et al.*, 1995] was used to calculate the water contents in pyrope-rich garnet. In addition, the absorption coefficient function of [Paterson, 1982] was also used to calculate the water contents. The calibration of Paterson [1982] is strongly dependent on the wavenumber, with a stronger contribution from wavenumbers closer to 3780 cm^{-1} . Defining the region of integration is thus extremely important for such a quantitative study. The infrared spectra were integrated from $3300\text{ to }3700\text{ cm}^{-1}$. For pyrope-rich garnet, the water content obtained from the extinction coefficient of [Bell *et al.*, 1995] is approximately 2–3 times greater than the water content determined from the [Paterson 1982] calibration. The reason for this difference is not well understood and we use both calibrations to compare our results with others.

3. Results

[6] The water content in pyrope-rich garnet gradually increases with pressure (Table 1 and Figure 1b). Infrared spectra at high pressures exhibit a broad asymmetric band centered around 3630 cm^{-1} . Multiple bands are observed at low pressures. It is likely that these bands are broadened due to pressure induced hydrogen bonding at high-pressures resulting in asymmetric bands. Upon weakening of hydrogen bonding and associated proton disorder, asymmetric peaks split into multiple bands [Geiger *et al.*, 1991]. Low energy bands between $3200\text{ and }3400\text{ cm}^{-1}$ are often attributed to molecular water in rutile inclusions [Matsyuk *et al.*, 1998]. In experiments where evidence for melting was observed, the chemical compositions of pyrope-rich garnet crystals were significantly altered (Figure S1a and S1b). The magnesium and iron content in pyrope-rich garnet evolved as a function of pressure, and at high pressure pyrope became more magnesium rich [Irifune and Isshiki, 1998; Frost, 2003]. The silicon, aluminium and chromium contents in the pyrope, however, remained mostly unchanged. In a few experiments (e.g., K650: 6 GPa and 1373 K; Table S1 and Figures S1c and S1d) we find that the pyrope crystal exhibits a magnesium-rich external rim surrounding a core of unaltered composition. Such a variation in composition correlates with the variation in water content, the magnesium-rich rim exhibits significantly higher water content than the unaltered region. Since the chemical diffusion of cations in garnet is sluggish, the contrast in composition across the rim to the core is likely due to dissolution-precipitation.

[7] Unpolarized infrared spectra on the (010) plane of olivine were collected to constrain (Table 1) the water fugacity using the results by [Kohlstedt *et al.*, 1996]. In experiments where partial melting occurred, olivine crystals were often dissolved in the melt, which made it difficult to estimate the water fugacity (f_{H_2O}). The dilution of H_2O within the melt phase results in a lower activity of the water; hence in such cases we estimate the lower limit of the water solubility in pyrope. In fact, we found that the partition coefficient, $D_{H_2O}^{ol/py}$ is dependent on water fugacity: $D_{H_2O}^{ol/py} < 1$ at water-saturated conditions, whereas under saturated conditions, $D_{H_2O}^{ol/py} \sim 3$ (slightly lower than the predicted partition coefficient of around 5 based on the water

Table 1. High Pressure Annealing Experiments^a

Exp	P (GPa)	T (K)	Time (hrs)	Garnet Water Content (ppm wt)		Olivine Water Content Paterson		D ^{ol/gt}
				Bell	Paterson	ppm wt	H/10 ⁶ Si	
K640 ^b	9	1473	24	778	341	849	13520	2.50
K670	9	1373	48	99	72	57	901	0.79
K648 ^b	8	1373	24	1024	433	x	x	x
K650 ^{b,c}	6	1373	24	863	353	x	x	x
K650 ^{b,d}	6	1373	24	578	235	x	x	x
K657 ^b	7	1373	24	1017	585	x	x	x
K659	7	1373	24	127	38	7	110	0.18
K689	5	1373	5	400	200	48	762	0.14

^aExp, experiment number; P, pressure; T, temperature; and time, experimental run duration. Experiments where olivine crystals were dissolved are denoted by x; all experiments have f_{O_2} set by Ni-NiO buffer, except K659 (Fe-FeO buffer).

^bExperiments with presence of melt phase.

^cExperiments with high Mg# (rim).

^dExperiments with low Mg# (core).

solubility data on Dora Maira pyrope [Lu and Keppler, 1997]).

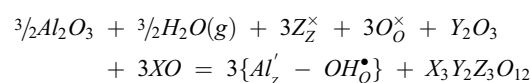
4. Discussion

[8] We detect no evidence of a diffusion profile for most of our samples and conclude that for most of our experiments the hydrogen content in our samples represents the equilibrium concentration. Such a result is consistent with the reported values of diffusion coefficients in pyrope of $\sim 10^{-10} \text{ m}^2/\text{s}^{-1}$ at 1373 K indicating the equilibration time scale is ~ 1 hour [Blanchard and Ingrin, 2004a, 2004b; Ingrin and Blanchard, 2006; Wang et al., 1996].

[9] We observe significantly higher water contents in pyrope-rich garnets compared to previous studies [Lu and Keppler, 1997; Withers et al., 1998]. At pressures >7 GPa, [Withers et al., 1998] reported an abrupt decrease in water content, whereas Lu and Keppler [1997] observed a small amount of water content (~ 200 ppm wt of H₂O). The abrupt decrease in water content is not consistent with any thermodynamic models of hydrogen dissolution [Keppler and Bolfan-Casanova, 2006]. At pressures <7 GPa, the water content reported by [Withers et al., 1998] is ~ 5 times higher than that reported by Lu and Keppler [1997] (Figure 2) and is similar to ours. A possible explanation for such a discrepancy might be related to subtle differences in the chemical composition. Trace amounts of boron (B) in tetrahedral sites and lithium (Li) in dodecahedral sites might form a coupled substitution with hydrogen [Lu and Keppler, 1997]. Lithium and boron impurities have been observed in olivine, however their concentration is much lower and there is no correlation between boron or lithium concentration with water content [Kent and Rossman, 2002]. Metasomatized garnet also contains these impurities [Paquin et al., 2004] and to our knowledge, any systematic correlation with water content is absent. The Li₂O + B₂O₃ content in our samples is of the order of 0.2 ppm wt compared to ~ 1000 ppm wt% reported by [Lu and Keppler 1997] and hence a coupled substitution between proton and these trace impurities is unlikely.

[10] A striking observation from our experiments is the large variation in water content in pyrope-rich garnet annealed at similar pressures and temperatures. Even at the same pressure (and similar temperature), the water content in garnet is very different between run K640 and

K670. In addition, in K650 the water content of the sample varies between the rim and the core where the Mg# is also different (see Figure S1). Because the pressure and temperature conditions are the same or similar in these samples, the cause of the variation in water content must be due to the difference in chemical environment. Based on the measurements of chemical composition (Table S1), we suggest that a possible parameter that affects the water content is Mg#. In addition, water fugacity may also cause such a difference (water fugacity inferred from water content in olivine was different among different runs, which is presumably due to the influence of melting and/or some water loss from the capsule). Therefore a combined effect of Mg# and water fugacity causes the difference in water content between K640 and K670 i.e., samples annealed at the same pressure and similar temperatures (temperature effect is corrected using the thermodynamic data). To make a quantitative analysis, we use a model in which the water content in garnet is proportional to $\exp(\alpha \cdot \text{Mg\#}) \cdot f_{H_2O}^r$. Values of α are determined from the data of experiment K650 where the water fugacity is likely the same between the rim and the core (because of fast diffusion), and is found to be 0.03. Applying this relation for the effect of Mg#, we combine the data from K640 and K670 to determine r to be ~ 0.4 . Although the above analysis is admittedly crude because of the paucity of data, the observed effect of Mg# and water fugacity are large and are likely to be real. We note that the sign of the Mg# effect inferred for garnet is opposite to that for olivine [Zhao et al., 2001]. Also, the fugacity exponent (r) inferred for garnet is smaller than that of olivine. The smaller value of r for pyrope compared to olivine explains the variation in the partition coefficient, $D_{H_2O}^{ol/py}$ with water fugacity. This value of r is also inconsistent with the hydrogarnet model which implies $r \sim 2$. In fact, if the hydrogarnet model for hydrogen dissolution in garnet were valid, then the dependence of hydrogen partitioning between olivine and garnet on water fugacity would be opposite to what we observed. A possible mechanism to explain this observation is the coupled substitution of silicon (Si⁴⁺) by a proton (H⁺) and aluminium (Al³⁺) [Hauri et al., 2006; Rauch and Keppler, 2002]. The chemical reaction



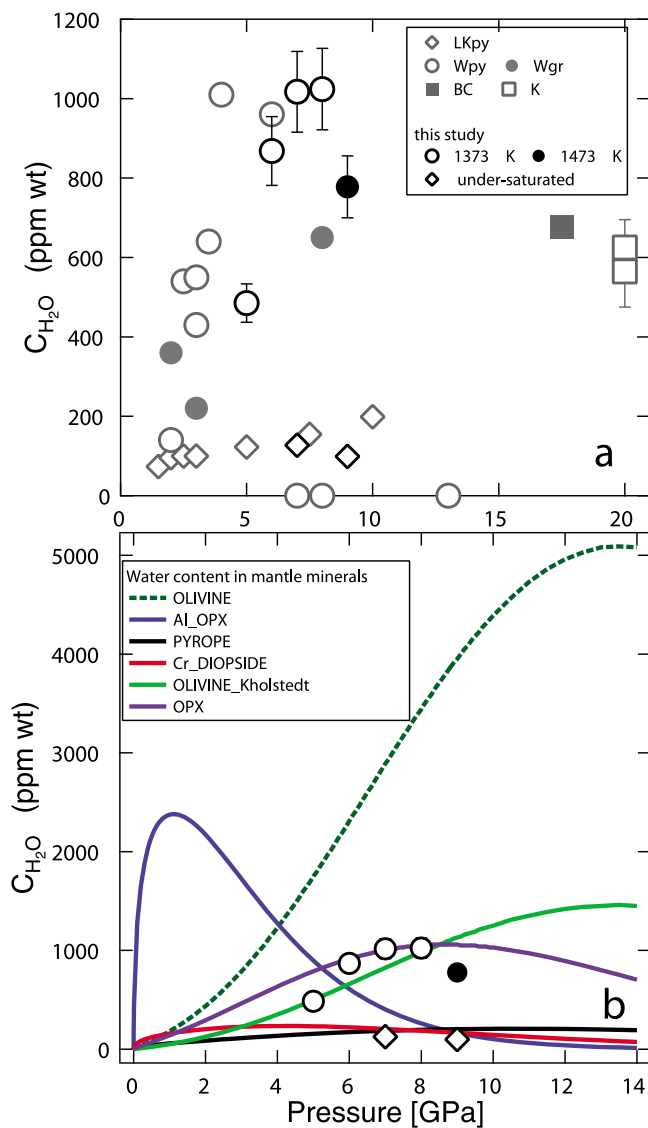


Figure 2. (a) Water content versus pressure in pyrope-rich garnet (Bell calibration). The black open circles, ($T \sim 1373$ K and $f_{O_2} \sim Ni-NiO$, time ~ 24 hrs except for 5 GPa (see Table 1); black filled circle, $T \sim 1473$ K and $f_{O_2} \sim Ni-NiO$; black open rhombs, undersaturated with respect to water; and data point at 7 GPa, $T \sim 1473$ K and $f_{O_2} \sim Fe-FeO$; grey open (pyrope) and filled (grossular) circles [Withers *et al.*, 1998], the grey rhombs [Lu and Keppeler, 1997], the filled square [Bolfan-Casanova *et al.*, 2000], and the open square [Katayama *et al.*, 2003] represent majorite. (b) Comparison of water solubility in various minerals in the upper mantle. The lines represent the thermodynamic model of water solubility for mantle minerals [Keppeler and Bolfan-Casanova, 2006], broken line for olivine shows the 3.5x [Kohlstedt *et al.*, 1996] model; open circles, filled circle, and rhombs are from present work. We have assumed 10% uncertainty associated with measurement of sample thickness and absorption coefficient of $\epsilon = 6700 \pm 670$ ($Lmol^{-1} cm^2$) [Bell *et al.*, 1995].

describes the coupled substitution and leads to $C_{OH} \propto f_{H_2O}^{1/2}$. The water fugacity exponent in this model is $1/2$ and is close to our observed value ($r \sim 0.4$). Note also that the water content increases with the activity of XO (X: Mg, Fe, Ca).

Higher Mg# possibly leads to enhanced vacancy concentration at the dodecahedral X-site, decreasing the activity of XO. Therefore this model is consistent with our observation of a positive correlation between water content and Mg#.

5. Geophysical Significance

[11] Some naturally occurring garnets contain water in excess of 1000 ppm wt [Xia *et al.*, 2005] which is inconsistent with previous experimental studies but could easily be explained by the present results. Garnets from the continental upper mantle of South Africa have lower water contents ~ 100 ppm wt or less [Bell *et al.*, 2004]. This is consistent with the view that continental mantle is depleted with incompatible components including water [Jordan, 1975; see also Karato, 2009]. [Bell *et al.*, 2004] reported a negative correlation between Mg# and the water content in garnet, which is contrary to our experiments on pyrope-rich garnet and controlled experiments on olivine by [Zhao *et al.*, 2001]. If a natural rock composition is modified by metasomatic fluids, the change in composition of rocks will be proportional to the degree of metasomatism, and various compositional parameters such as Mg#, water content and TiO_2 content will exhibit strong correlation reflecting the composition of the metasomatic fluid. Consequently, we propose that the observed trend reported by [Bell *et al.*, 2004] is due to varying extents of metasomatism by fluids rich in water, Fe and TiO_2 such as kimberlite magma [Wedepohl and Muramatsu, 1979]. The TiO_2 content reported by [Xia *et al.*, 2005] is similar to our sample and closer to a typical upper mantle composition, whereas [Bell *et al.*, 2004] reported higher TiO_2 contents suggesting the influence of metasomatism. This model implies that unaltered continental upper mantle would contain less water (less than 100 ppm wt), which is consistent with its longevity that requires a much higher viscosity than the surrounding mantle [Lenardic and Moresi, 1999; Shapiro *et al.*, 1999].

[12] The present results provide a new data set to discuss water transport by garnet. The bulk of the subducted oceanic crust in the deep upper mantle is made of pyrope-rich garnet [Irfune and Ringwood, 1987]. Hence, the maximum amount of water transported by pyrope-rich garnet in the subducted oceanic crust is $\sim 3 \times 10^{11}$ kg/year. This is roughly the half of the estimated water flux associated with the igneous components of subducted oceanic crust [Jarrard, 2003]. Substantially higher water solubility in pyrope-rich garnet might affect the relative strength of garnet with respect to other mineral phases such as olivine [Katayama and Karato, 2008]. In addition, hydrogen defects in pyrope-rich garnet also affect electrical conductivity [Dai and Karato, 2009b].

[13] **Acknowledgments.** Thoughtful reviews by D. J. Frost and two anonymous reviewers are greatly appreciated. Authors thank Eizo Nakamura (ISEI, Misasa) for the chemical analyses of B and Li. This work was supported by the U.S. National Science Foundation.

References

- Bell, D. R., *et al.* (1995), Quantitative analysis of trace OH in garnet and pyroxenes, *Am. Mineral.*, 80, 465–474.
 Bell, D. R., *et al.* (2004), Abundance and partitioning of OH in a high-pressure magmatic system: Megacrysts from the Monastery kimberlite, South Africa, *J. Petrol.*, 45, 1539–1564, doi:10.1093/petrology/egh015.

- Blanchard, M., and J. Ingrin (2004a), Hydrogen diffusion in Dora Maira pyrope, *Phys. Chem. Miner.*, *31*, 593–605, doi:10.1007/s00269-004-0421-z.
- Blanchard, M., and J. Ingrin (2004b), Kinetics of deuteration in pyrope, *Eur. J. Mineral.*, *16*, 567–576, doi:10.1127/0935-1221/2004/0016-0567.
- Bolfan-Casanova, N., et al. (2000), Water partitioning between nominally anhydrous minerals in the MgO-SiO₂-H₂O system up to 24 GPa: Implications for the distribution of water in the Earth's mantle, *Earth Planet. Sci. Lett.*, *182*, 209–221, doi:10.1016/S0012-821X(00)00244-2.
- Bromiley, G. D., et al. (2004), Hydrogen solubility and speciation in natural, gem quality chromian diopside, *Am. Mineral.*, *89*, 941–949.
- Dai, L., and S. Karato (2009a), Electrical conductivity of pyrope-rich garnet at high temperature and pressure, *Phys. Earth Planet. Inter.*, *176*, 83–88, doi:10.1016/j.pepi.2009.04.002.
- Dai, L., and S. Karato (2009b), Electrical conductivity of orthopyroxene: Implications for the water content of the asthenosphere, *Proc. Jpn. Acad.*, in press.
- Dai, L., and S. Karato (2009c), Electrical conductivity of wadsleyite under high pressures and temperatures, *Earth Planet. Sci. Lett.*, *287*, 277–283, doi:10.1016/j.epsl.2009.08.012.
- Frost, D. J. (2003), Fe²⁺-Mg partitioning between garnet, magnesio-wüstite, and (Mg,Fe)₂SiO₄ phases of the transition zone, *Am. Mineral.*, *88*, 387–397.
- Geiger, C. A., et al. (1991), The hydroxide component in synthetic pyrope, *Am. Mineral.*, *76*, 49–59.
- Hauri, E. H., et al. (2006), Partitioning of water during melting of the Earth's upper mantle at H₂O-undersaturated conditions, *Earth Planet. Sci. Lett.*, *248*, 715–734, doi:10.1016/j.epsl.2006.06.014.
- Hirschmann, M. M., et al. (2005), Storage capacity of H₂O in nominally anhydrous minerals in the upper mantle, *Earth Planet. Sci. Lett.*, *236*, 167–181, doi:10.1016/j.epsl.2005.04.022.
- Huang, X., et al. (2005), Water content of the mantle transition zone from the electrical conductivity of wadsleyite and ringwoodite, *Nature*, *434*, 746–749, doi:10.1038/nature03426.
- Ingrin, Y., and M. Blanchard (2006), Diffusion of hydrogen in minerals, in *Water in Nominally Anhydrous Minerals*, edited by H. Keppler and J. R. Smyth, pp. 291–302, Mineral. Soc. of Am., Washington, D. C.
- Irfune, T., and M. Isshiki (1998), Iron partitioning in a pyrolite mantle and the nature of the 410-km seismic discontinuity, *Nature*, *392*, 702–705, doi:10.1038/33663.
- Irfune, T., and A. E. Ringwood (1987), Phase transformations in a harzburgite composition to 26 GPa: Implications for dynamical behaviour of the subducting slab, *Earth Planet. Sci. Lett.*, *86*, 365–376, doi:10.1016/0012-821X(87)90233-0.
- Jacobsen, S. D., and J. R. Smyth (2006), Effect of water on the sound velocities of ringwoodite in the transition zone, in *Earth's Deep Water Cycle*, *Geophys. Monogr. Ser.*, vol. 168, edited by S. D. Jacobsen and S. van der Lee, pp. 131–145, AGU, Washington, D. C.
- Jarrard, R. D. (2003), Subduction fluxes of water, carbon dioxide, chlorine, and potassium, *Geochem. Geophys. Geosyst.*, *4*(5), 8905, doi:10.1029/2002GC000392.
- Jordan, T. H. (1975), The continental tectosphere, *Rev. Geophys. Space Phys.*, *13*, 1–12, doi:10.1029/RG013i003p00001.
- Jung, H., and S. Karato (2001), Water-induced fabric transitions in olivine, *Science*, *293*, 1460–1463, doi:10.1126/science.1062235.
- Karato, S. (2009), Rheology of the deep upper mantle and its implications for the preservation of the continental roots: A review, *Tectonophysics*, in press.
- Katayama, I., and S. Karato (2008), Effects of water and iron content on the rheological contrast between garnet and olivine, *Phys. Earth Planet. Inter.*, *166*, 59–66.
- Katayama, I., K. Hirose, H. Yurimoto, and S. Nakashima (2003), Water solubility in majorite garnet in subducting oceanic crust, *Geophys. Res. Lett.*, *30*(22), 2155, doi:10.1029/2003GL018127.
- Kent, A. J. R., and G. R. Rossman (2002), Hydrogen, lithium, and boron in mantle-derived olivine: The role of coupled substitution, *Am. Mineral.*, *87*, 1432–1436.
- Keppler, H., and N. Bolfan-Casanova (2006), Thermodynamics of water solubility and partitioning, in *Water in Nominally Anhydrous Minerals*, edited by H. Keppler and J. R. Smyth, pp. 193–230, Mineral. Soc. of Am., Washington, D. C.
- Kohlstedt, D. L., et al. (1996), Solubility of water in the α , β and γ phases of (Mg,Fe)₂SiO₄, *Contrib. Mineral. Petrol.*, *123*, 345–357, doi:10.1007/s004100050161.
- Kushiro, I., Y. Syono, and S.-I. Akimoto (1968), Melting of a peridotite nodule at high pressures and high water pressures, *J. Geophys. Res.*, *73*, 6023–6029, doi:10.1029/JB073i018p06023.
- Lenardic, A., and L. N. Moresi (1999), Some thoughts on the stability of cratonic lithosphere: Effects of buoyancy and viscosity, *J. Geophys. Res.*, *104*, 12,747–12,759, doi:10.1029/1999JB900035.
- Lu, R., and H. Keppler (1997), Water solubility in pyrope to 100 kbar, *Contrib. Mineral. Petrol.*, *129*, 35–42, doi:10.1007/s004100050321.
- Mackwell, S. J., D. L. Kohlstedt, and M. S. Paterson (1985), The role of water in the deformation of olivine single crystals, *J. Geophys. Res.*, *90*, 11,319–11,333, doi:10.1029/JB090iB13p11319.
- Matsyuk, S. S., et al. (1998), Hydroxyl defects in garnets from mantle xenoliths in kimberlites of the Siberian platform, *Contrib. Mineral. Petrol.*, *132*, 163–179, doi:10.1007/s004100050414.
- Mierdel, K., et al. (2007), Water solubility in aluminous orthopyroxene and the origin of Earth's asthenosphere, *Science*, *315*, 364–368, doi:10.1126/science.1135422.
- Paquin, J., et al. (2004), Li-Be-B systematics in the ultrahigh-pressure garnet peridotite from Alpe Arami (central Swiss Alps): Implications for slab-to-mantle wedge transfer, *Earth Planet. Sci. Lett.*, *218*, 507–519, doi:10.1016/S0012-821X(03)00677-0.
- Paterson, M. S. (1982), The determination of hydroxyl by infrared absorption in quartz, silicate glass and similar materials, *Bull. Mineral.*, *105*, 20–29.
- Rauch, M., and H. Keppler (2002), Water solubility in orthopyroxene, *Contrib. Mineral. Petrol.*, *143*, 525–536.
- Shapiro, N., et al. (1999), Stability and dynamics of the continental tectosphere, *Lithos*, *48*, 135–152, doi:10.1016/S0024-4937(99)00027-4.
- Wang, D., et al. (2006), The effect of water on the electrical conductivity in olivine, *Nature*, *443*, 977–980, doi:10.1038/nature05256.
- Wang, L., et al. (1996), Diffusion of the hydrous component in pyrope, *Am. Mineral.*, *81*, 706–718.
- Wedepohl, K. H., and Y. Muramatsu (1979), The chemical composition of kimberlites compared with the average composition of three basaltic magma types, in *Kimberlites, Diatremes, and Diamonds: Their Geology, Petrology, and Geochemistry*, edited by F. R. Boyd and H. O. A. Meyer, pp. 300–312, AGU, Washington, D. C.
- Withers, A. C., et al. (1998), The OH content of pyrope at high pressure, *Chem. Geol.*, *147*, 161–171, doi:10.1016/S0009-2541(97)00179-4.
- Xia, Q. K., et al. (2005), Heterogeneity of water in garnet from UHP eclogites, eastern Dabie Shan, China, *Chem. Geol.*, *224*, 237–246, doi:10.1016/j.chemgeo.2005.08.003.
- Zhao, Y.-H., et al. (2001), Experimental investigation on water solubility in olivine single crystal with different Fe content, *Acta Petrol. Sin.*, *17*, 123–128.

S. Karato, Department of Geology and Geophysics, Yale University, New Haven, CT 06520, USA.

M. Mookherjee, Bayerisches Geoinstitut, University of Bayreuth, Bayreuth, D-95440 Germany. (mainak.mookherjee@uni-bayreuth.de)